

Dynamics of solid inner-shell electrons in collisions with bare and dressed swift ionsC. C. Montanari,¹ J. E. Miraglia,^{1,2} and N. R. Arista^{3,4}¹*Instituto de Astronomía y Física del Espacio (Conicet), Casilla de Correo 67, Sucursal 28, 1428 Buenos Aires, Argentina*²*Departamento de Física, FCEyN, Universidad de Buenos Aires, Buenos Aires, Argentina*³*Instituto Balseiro, Centro Atómico Bariloche, 8400 Bariloche, Argentina*⁴*Universidad Nacional de Cuyo, Bariloche, Argentina*

(Received 11 April 2002; published 22 October 2002)

We analyze the dynamical interactions of swift heavy projectiles and solid inner-shell electrons. The dielectric formalism employed to deal with the free-electron gas is extended to account for the core electrons, by using the local plasma approximation. Results for stopping power, energy straggling, and inner-shell ionization in collisions of bare ions with metals are displayed, showing very good accord with the experimental data. Simultaneous excitations of projectile and target electrons are also analyzed. In the high-energy range we find a similar contribution of target core and valence electrons to the probability of projectile-electron loss. The problem of no excitation threshold within the local plasma approximation and the possibility of collective excitations of the shells are discussed.

DOI: 10.1103/PhysRevA.66.042902

PACS number(s): 34.50.Bw, 31.70.-f

I. INTRODUCTION

The dynamics of atomic particles traveling through solid matter is basic to atomic physics and material sciences, being of great interest because of its technological applications. The interactions of swift heavy projectiles with dense media have been extensively analyzed, especially by considering the interaction with the solid free-electron gas (FEG) [1–7]. A complete description of the media must also include the screened nuclei and the core or inner-shell electrons (ISE). The usual approximation consists of assuming that ISE are frozen and only valence electrons react to the external excitation. The calculation of the response of the whole electronic system of the solid is a difficult many-body problem. A detailed study on the effect of the combined core-valence electrons on the dielectric response of simple metals has been developed by Sturm, Zaremba, and Nuroh [8] by considering ISE polarization.

In recent years, the description of the interaction of projectiles and solid ISE has attracted interest, mainly related to stopping-power calculations in high-velocity collisions, where the contribution of the ISE proved to be more important than the FEG [9]. Also important is the role played by target ISE in the substate mixing of the projectile [10,11].

The problem of the interaction of ions with the bound electrons of matter has received considerable theoretical effort in the past decades [8,12–16]. One of the theoretical descriptions of the ISE response to the interaction with fast heavy ions is the local plasma approximation (LPA) [17–19]. There have been many applications of this model, from the original proposal of Linhard and co-worker [17] to more recent contributions for stopping-power calculations by deep bound electrons [20], or coupling of projectile-orbitals by the induced potential [18], providing results in accord with the experimental measurements.

In previous works we obtained probabilities of inelastic processes in the projectile (excitation and electron loss) due to the interaction with the screened target nucleus [21] and with the solid FEG [22]. In the present contribution we con-

sider the dynamics of both target and projectile bound electrons. The main purpose of this work is to examine the contribution of ISE to projectile-electron excitation and loss at intermediate to high impact velocities ($v \gtrsim Z_p$). We are interested in the description of processes with simultaneous excitation of the projectile and the target electrons. We will employ a combination of the LPA (for target-electron excitations) and the first Born approximation (for projectile-electron ones).

The work is organized as follows. In Sec. II we briefly summarize the theoretical model employed. In Sec. III we present the results related to three items. In the first one, we analyze the influence of target ISE in collisions of bare projectiles with metals. Results of stopping power, energy straggling, and inner-shell ionization are displayed and compared with a large variety of experimental data. In the second part of Sec. III we present the inelastic contribution of ISE to projectile-electron excitation and loss. In the third one, the LPA distribution in the energy gained by the target electrons is investigated. The problem of no excitation threshold within the LPA [16,19,23] is discussed.

The atomic units system will be used throughout this work.

II. THEORY

We consider the interaction of fast projectiles (of nuclear charge Z_p and impact velocity v) with all the solid electrons (ISE and FEG). We extend the dielectric formalism employed to deal with the FEG to account for the ISE by using the LPA. Summarizing, this model assumes two approximations. First, bound electrons react to the external perturbation as free particles, which can be described at each point of space \vec{r} as belonging to a FEG with a local Fermi velocity $k_F(r) = [3\pi^2 n(r)]^{1/3}$, where $n(r)$ is the electronic density. Second, the corresponding dielectric function is a spatial mean value of the Linhard dielectric function $\varepsilon(q, \omega, k_F(r))$ [18]

$$\frac{1}{\varepsilon^{LPA}(q, \omega)} = \frac{3}{R_{WS}^3} \int_0^{R_{WS}} r^2 dr \frac{1}{\varepsilon(q, \omega, k_F(r))}, \quad (1)$$

with R_{WS} being the Wigner-Seitz sphere radius [$R_{WS} = [3/(4\pi n_{at})]^{1/3}$ and n_{at} the solid atomic density].

The LPA satisfies the f -sum rule as far as the correct density of electrons is used. It is

$$\begin{aligned} N_e &= \frac{1}{2\pi^2 n_{at}} \int_0^\infty \omega d\omega \text{Im} \left[\frac{-1}{\varepsilon^{LPA}(q, \omega)} \right] \\ &= \frac{1}{2\pi^2 n_{at}} \int_0^\infty \omega d\omega \text{Im} [\varepsilon^{LPA}(q, \omega)], \end{aligned} \quad (2)$$

where $N_e = 3/R_{WS}^3 \int_0^{R_{WS}} dr r^2 n(r)$ is the total number of bound electrons. Equation (2) assures the correct high-velocity limit for the stopping power.

It is useful to remark here that the LPA [17–20] considers target bound electrons as a FEG. It implies that any value of energy gained by these electrons, $\omega > 0$, is allowed, not only the values greater than the nl -shell binding energy ϵ_{nl} . Hereafter we will refer to the energy region $0 < \omega < \epsilon_{nl}$ as the below ionization energy region (BIER). The question about the physical meaning of the energy transferred to the target electrons below the ionization threshold is a conflicting point of the model and, probably, the major set back of the LPA. However, the LPA verifies the f -sum rules and gives the correct high-energy limit for the stopping power as given in Eq. (2) only if we integrate the energy gained by any target electron from $\omega = 0$. If we cut off the values below the ionization threshold, the f -sum rule and the high-velocity limit is not fulfilled any more.

III. RESULTS

As a first step we apply the LPA to calculate the response of the ISE in collisions of *bare* ions with the solid target. In this way we single out the performance of the approximation to deal with target-electron excitations, and compare the theoretical results with the large variety of experimental data available for protons colliding with Al, Si, and Cu. Afterwards, we deal with *dressed* projectiles and employ the LPA to describe the response of the ISE of the solid to the projectile-electron promotion: either excitation or electron loss.

The spatially dependent densities $n(r)$ of the ISE for *each* shell are obtained from the Hartree-Fock wave functions of the target [24]. It allows us to consider either *each* shell separately, or the *whole* set of ISE by adding the shell densities. When evaluating the contribution of the ISE, we include all the bound electrons, i.e., K and L shells for aluminum and silicon, and K , L , and M shells for copper. Even when the contribution of the deeply bound electrons (i.e., K -shell electrons) is negligible at intermediate velocities, it is important to check the proper high-velocity limit.

Apart from the ISE response to the collision, the FEG contribution is calculated in the usual way [22,25] within the dielectric formalism, by employing the Mermin-Linhard di-

electric function [26] for a gas of electrons of homogeneous density. The parameters employed to characterize the FEG are the number of valence electrons N_e , the radius of the Seitz cell per electron r_s , and the damping rate of the plasmons γ . That is $N_e = 3$, $r_s = 2.10$, and $\gamma = 0.037$ for Al; $N_e = 4$, $r_s = 1.98$, and $\gamma = 0.156$ for Si; $N_e = 2$, $r_s = 2.12$, and $\gamma = 1.2$ for Cu [27,28].

A. Collisions of bare ions with metals

In the case of bare projectiles colliding with solids, the moments of the energy loss of order j read [19]

$$W_j = \frac{2Z_P^2}{\pi v^2} \int_0^\infty \frac{dq}{q} \int_0^{qv} \text{Im} \left[-\frac{1}{\varepsilon^{LPA}(q, \omega)} \right] \omega^j d\omega. \quad (3)$$

In particular, W_0 is the probability, $W_1 = S$ is the stopping power, W_2 is the energy straggling, all of them expressed per unit length. Results of applying the LPA to the calculation of these three energy moments are reported next.

1. Stopping power

In Fig. 1 we display *total* stopping power per unit length, FEG and ISE contributions summed up, in collisions of protons with Al, Si, and Cu. Our LPA curve is plotted together with the experimental data and with the results of the semi-empirical model of Abril *et al.* [9]. The latter is a combination of Mermin-type dielectric functions with parameters that fit the experimental optical properties of each solid.

The agreement of the LPA with the experiments is good. The LPA overestimates the data by few percents near the maximum for Al and Si targets. In these cases the main contribution comes from the excitation of the L shell, whose electronic velocity is $v_e \approx 3$ a.u. For impact velocity $v \geq v_e$ the agreement with the data is surprisingly good. For Cu, the dispersion of the experimental results at intermediate velocities is greater than for the other targets and our results seem to have a better performance as compared with a group of experimental data. Near the maximum, the main contribution for Cu comes from the $3d$ state, which is more liable to be approximated as a FEG, since it has small binding energy ($\epsilon_{3d} \approx -0.74$ a.u. and $v_e \approx 1.2$ a.u. [24]).

In all the cases, the LPA curves have the correct high-velocity limit, expressed by Eq. (2). This behavior is related to the fact that we include the whole set of target electrons considering even the K shell. Anyway, in our range of energy, the main contribution comes from the outer shells (L shell for Al and Si, M shell for Cu) and, of course, the FEG.

The importance of including in the stopping power those excitations inside the BIER depends on the projectile velocity. For example, in collisions of protons with Al at impact velocity $v = 6$ a.u., the contribution of the BIER represents 10% of the total stopping power. This velocity is inside the high-velocity region of Fig. 1, where the agreement with the experimental data is very good. The question is the physical sense of energy absorbed by bound electrons lower than the ionization threshold. We will return to this point later.

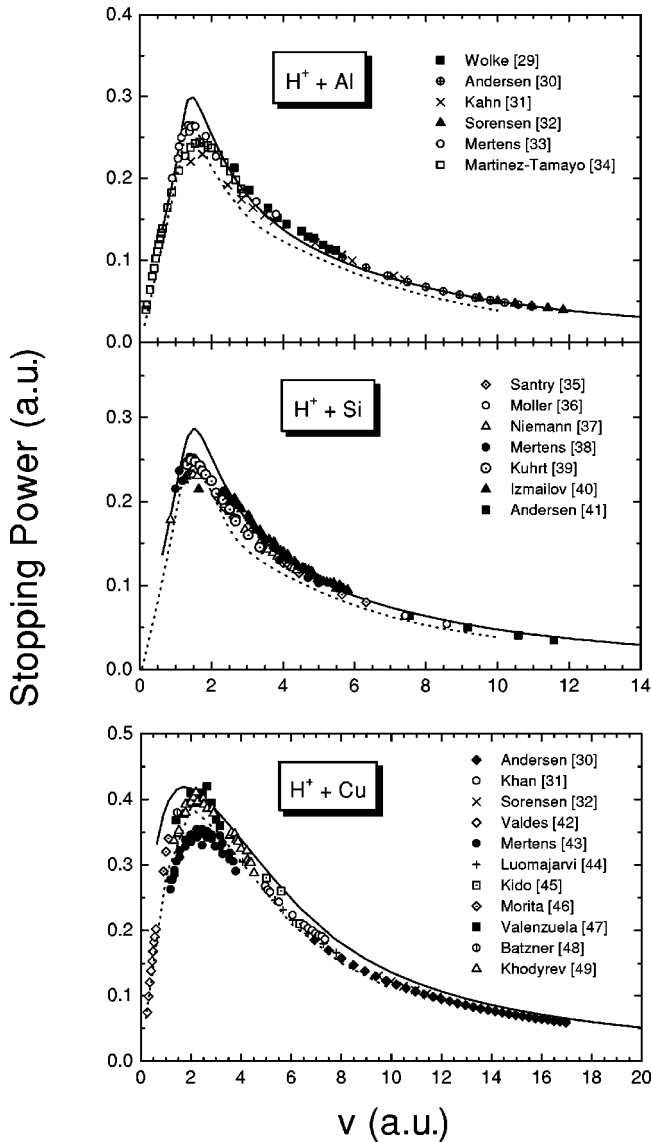


FIG. 1. Total stopping power in collisions of protons with different metals, ISE and FEG contributions summed up. Notation: solid line, present LPA calculations; dotted line, semiempirical results of Abril *et al.* [9]. Experimental data: Refs. [29–49].

2. Energy straggling

Figure 2 shows energy straggling Ω of protons in the same targets, Al, Si, and Cu, as function of the impact energy. The energy straggling is defined as $\Omega = \sqrt{W_2}$, where W_2 is given by Eq. (3). The values obtained are normalized to the Bohr straggling Ω_B ,

$$\Omega_B = \sqrt{4\pi Z_p^2 Z_T n_{at}}. \quad (4)$$

In this figure we plot two theoretical curves, total energy straggling including the ISE and the FEG, and the FEG contribution alone. The well-known saturation effect is observed in the FEG curve at high velocities. This highlights the important role played by ISE to reproduce the experimental data. Note that the asymmetric error bars in the results of

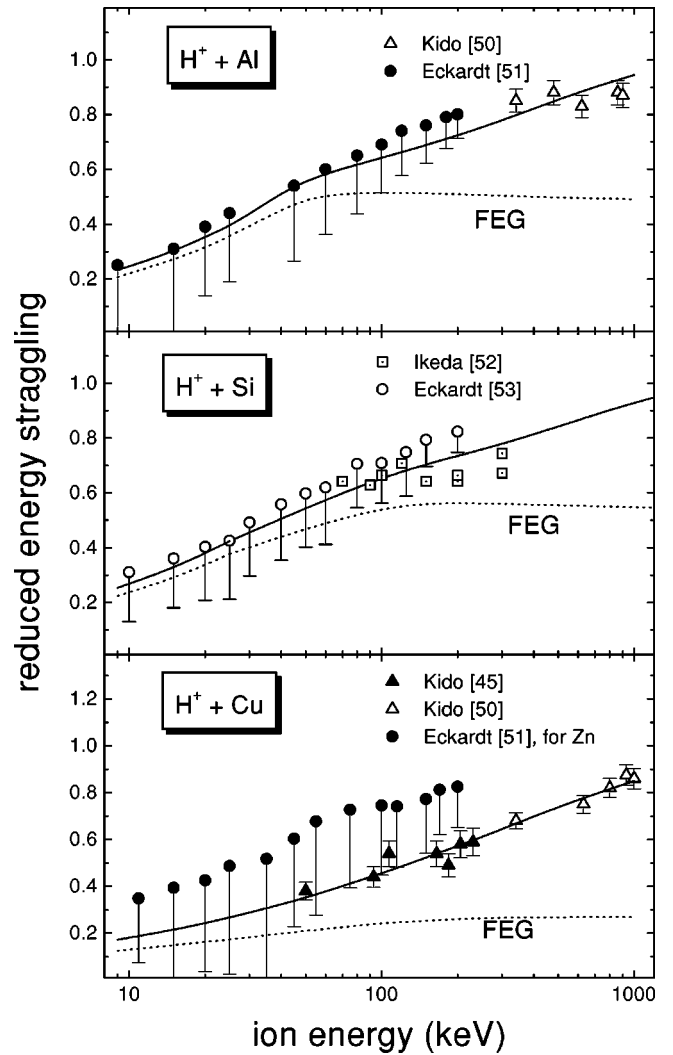


FIG. 2. Energy straggling from Eq. (3) normalized to the Bohr straggling Ω_B given by Eq. (4). Notation: solid line, present LPA calculations considering all target electrons (ISE and FEG); dotted line, only the FEG contribution. Experimental data: Refs. [45,50–53].

Eckardt and co-workers [51,53], included in Fig. 2, are the maximum correction for the foil roughness. The agreement between our LPA results and the experiments is good even at low velocities.

The straggling is related to the second momentum of the energy. The integration over ω in Eq. (3) depends strongly on the values of $\text{Im}[-1/\epsilon^{LPA}(q, \omega)]$ at low ω . This is a very sensitive region for any theoretical model to describe the process properly. For energy moments W_j , with $j \geq 1$, the term ω^j masks the behavior of the probability at small ω . When we evaluate energy straggling, the factor ω^2 loses the form of the function at low ω , retaining only the Coulomb tail. The agreement of the LPA shown in Fig. 2 even at low velocities is reasonable. On the contrary, probabilities per unit length $P = W_0 = 1/\lambda$, (with λ being the mean free path) are the most sensitive magnitudes since they precisely sample the region very close to $\omega = 0$.

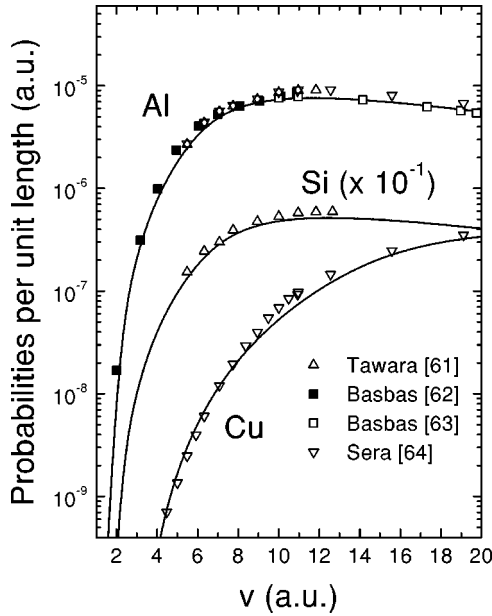


FIG. 3. K -shell ionization of Al, Si, and Cu by protons. Notation: solid line, LPA calculations. Experimental data: Refs. [61–64].

3. Inner-shell ionization

One particular magnitude to inspect is the ionization probability. In the past decades inner-shell ionization processes have received much attention as shown by the compilations of Orlic and co-workers [54,55], Braziewicz and co-workers [56,57], Paul and co-workers [58,59], and Lapicki [60]. A large variety of experimental data is tabulated and available in the literature and may be used for comparison [61–66].

The LPA as presented here is specially suitable in the calculation of inner-shell ionization cross sections. We can evaluate each shell separately and take into account the gap (ionization energy), shell to shell. In this case we do know that the final state of the target-electron satisfies the condition $\omega > \epsilon_{nl}$. We impose this condition on the LPA by integrating the contribution of each shell in Eq. (3) from $\omega = \epsilon_{nl}$. The values of orbital energies are given by the Hartree-Fock tables [24].

In Fig. 3 we test the model for K -shell ionization of Al, Si, and Cu by protons. Probabilities per unit length are obtained as a product of the cross section times the atomic density of the target, n_{at} . The comparison with the experimental results is surprisingly good. We have also successfully tested the model for K -shell ionization of ISE of many other collisional systems, not reported here.

In Fig. 4 we display LPA results for L -shell ionization of Si by protons. K -shell results are also plotted for comparison. The L -shell ionization is at least two orders of magnitude more important than the K -shell ionization, so the L -shell curve plotted in Fig. 4 is closed to the total ionization one. Again, the agreement between theory and experiments is good, though our L -shell curve runs below the experiments. The LPA ionization values are sensitive to the shell binding energy considered. Any difference in this energy is more significant for the L shell (small binding energy) than for the K shell.

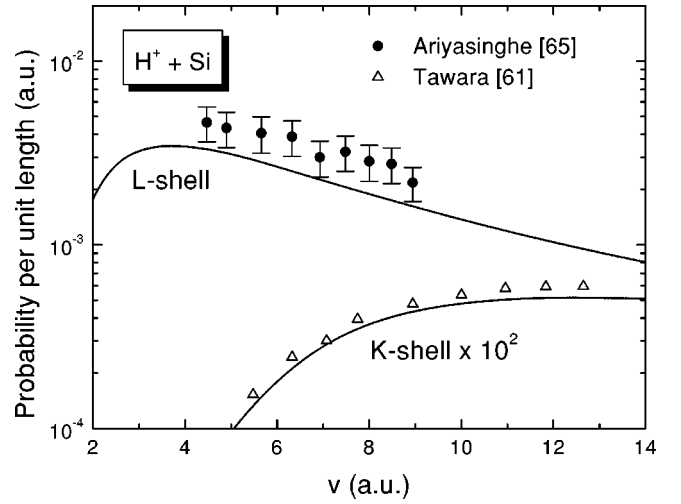


FIG. 4. LPA probabilities per unit length of L - and K -shell ionization of Si by protons as a function of the impact velocity. Experimental data: Refs. [61,65].

B. Collisions of dressed projectiles with metals

In this section we focus on projectile inelastic processes due to the interaction with all the electrons of the metal. The participation of target ISE in these processes can take place in two ways: frozen in the same state with their role restricted to screening the nuclear charge, or active when the target ISE are excited. This simultaneous excitation of projectile and target electrons is the antiscreening effect, of well-known importance in collisions with gases [67–75]. In a previous work [21] we have calculated projectile-electron excitation and loss by considering only the screening role of the target electrons. In the present contribution our aim is to consider solid antiscreening mechanisms by using the LPA. This is a field where the LPA can become an important and useful tool because a direct atomic calculation involves the determination of several target atomic factors and the corresponding sums. Instead, the LPA considers any final excited state as a whole.

The energy moments for excitation processes of dressed projectiles read [22]

$$W_j^{exc}(i,f) = \frac{2}{\pi v^2} \int_{\Delta\epsilon/v}^{\infty} \frac{dq}{q} \int_0^{qv-\Delta\epsilon} F_{if}(q,\omega) \times \text{Im} \left[-\frac{1}{\epsilon^{LPA}(q,\omega)} \right] (\omega + \Delta\epsilon)^j d\omega, \quad (5)$$

with $\Delta\epsilon = \epsilon_f - \epsilon_i$ being the energy gained by the projectile electron excited from the initial state i to the final state f , and $F_{if}(q,\omega)$ being the atomic form factor of the hydrogenic projectile considering unperturbed initial and final wave functions (first Born approximation).

For projectile-electron-loss processes, the final state is characterized by $f = \vec{k}$, the electron momentum with respect

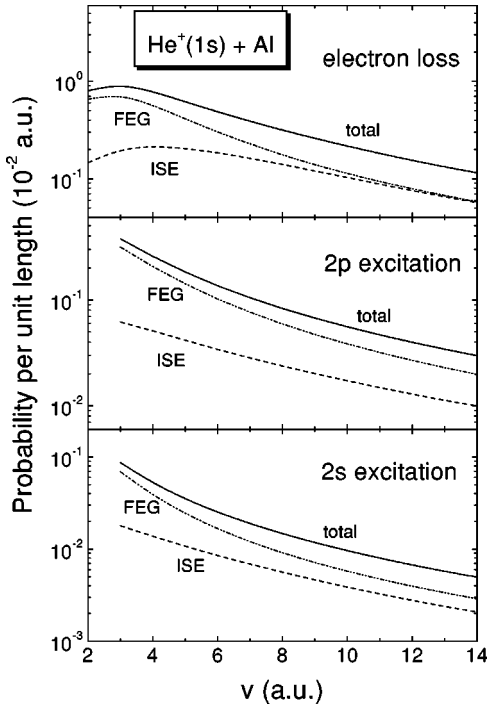


FIG. 5. Electron excitation and loss probabilities per unit length in $\text{He}^+(1s) + \text{Al}$ collisions. They are obtained by using the present LPA together with the first Born approximation for the projectile form factor. Partial ISE and FEG contributions are plotted separately, and sum up to give total probabilities.

to the ion. The moments $W_j^{loss}(i, \vec{k})$ require an additional integration on \vec{k} . In this case the energy gained by the projectile electron depends on the momentum of the electron as $\Delta\epsilon = k^2/2 - \epsilon_i$. The projectile ionization form factor, $F_{i\vec{k}}(q, \omega)$, is calculated in first Born approximation in the usual way [76–81], with the loss electron described by the Coulomb wave function in the continuum of the projectile.

We consider hydrogenic projectiles He^+ colliding with Al at intermediate to high velocities. The dynamical screening of the ion by the FEG is taken into account [82]. The consequence of this screening is that the binding energies inside the solid are relaxed depending on the ion velocity. For instance, there is no He^+ ($n=2$) bound state for $v < 3$ a.u. [22,83]. For very high impact velocity, the electrons of the FEG cannot respond to the ion perturbation, and the binding energies inside the solid tend to those of the isolated hydrogenic atom.

Figure 5 displays the probabilities per unit length for projectile-electron excitation $1s \rightarrow 2p$, $1s \rightarrow 2s$, and for electron loss. The FEG and ISE contributions are plotted separately and summed up as total probabilities. The electron-loss process is the main inelastic transition, and the only one for $v < 3$ a.u. Also important is the $2p$ excitation, which is nearly one order of magnitude larger than $2s$ excitation.

As can be observed in Fig. 5, the contribution of the excitation of ISE to the processes studied is appreciable even at intermediate velocities. We define the ratio of probabilities as follows:

$$R = P_{ISE} / (P_{FEG} + P_{ISE}), \quad (6)$$

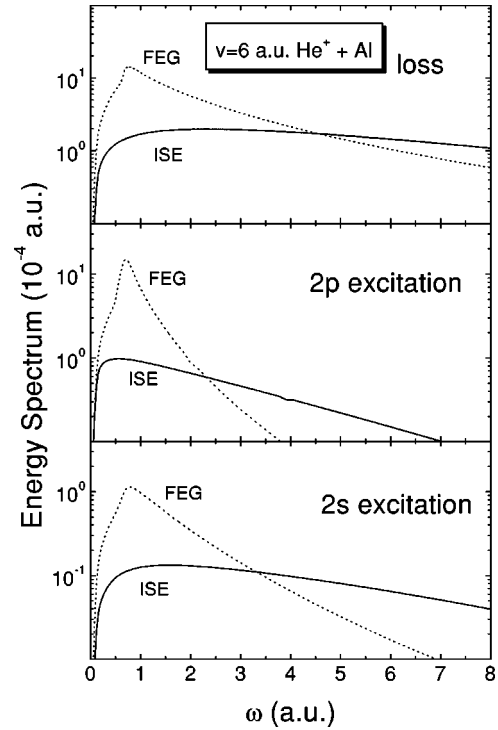


FIG. 6. Probabilities per unit length for $\text{He}^+(1s)$ inelastic transitions as a function of the energy gained by the target electron.

where P_{ISE} and P_{FEG} are probabilities per unit length due to the interaction with the ISE and the FEG, respectively. For electron loss of He^+ projectiles at impact velocity $v = 6$ a.u., $R = 0.4$, and $R \rightarrow 0.5$ for higher velocities. This means equipartition of the aluminum ISE and FEG contribution. For $2p$ and $2s$ excitation of He^+ , P_{ISE} are also comparable to P_{FEG} as seen from Fig. 5. This brings us again to the importance of the antiscreeing effect. For gases it has been found that target-electron excitation (antiscreeing) contributes significantly to projectile-electron excitation as compared with screening mechanisms [67–75]. Therefore, it is not enough to consider the bound electrons of the target atoms as frozen observers: their dynamics plays an important role. The same role is found here for solids by using the LPA.

C. Dependence on the energy gained by target electrons

We evaluate probabilities per unit length as a function of the energy gained by the metal electrons, $dW_0/d\omega$, and plot the corresponding energy spectra. Figure 6 shows energy spectra in the processes of projectile excitation or loss due to the interaction with the FEG and the ISE. The probabilities due to the interaction of He^+ with the aluminum FEG show a peak at $\omega \approx 0.65$ a.u., which is the known plasmon peak (collective excitations of the FEG) shifted due to the dispersion relation [22]. The energy absorbed by the ISE is not so localized as that of the FEG due to the spatial mean value done within the LPA. Note that the importance of He^+ excitation $1s \rightarrow 2p$ is comparable to that of the electron loss, not so the $1s \rightarrow 2s$ excitation.

We have an important contribution to total LPA probabilities from the BIER (i.e., for Al, $\varepsilon_{2p} \approx -4.5$ a.u.). It represents (probably unphysical) single-electron excitations or even collective modes of excitation of the bound shells, if any. The comparison with the experimental data realized for stopping power or energy straggling in preceding sections leaves the possibility open. As we mentioned before, we do include energies belonging to the BIER in these calculations. Anyway, the BIER contribution is lower for energy moments W_1 or W_2 than for W_0 .

IV. CONCLUSIONS

In this contribution we deal with the role of the dynamics of solid ISE in collisions with bare ions and hydrogenic projectiles at intermediate to high velocities. We extend the dielectric formalism employed to deal with the FEG, to account for the ISE by using the LPA. This model describes the ISE as a FEG of local dependent density. The electronic densities of each atomic shell are obtained from the corresponding Hartree-Fock wave functions.

This formalism allows us to calculate stopping power, energy straggling, and probabilities per unit length for bare projectiles colliding with the whole electronic system of some metals, such as Al, Si, and Cu. The comparison of the LPA results and the experimental data available is surprisingly good. We also test the LPA to deal with inner-shell

ionization by circumscribing the jump in energy gained by the electrons to values greater than the shell binding energy. *K*-shell and *L*-shell ionization probabilities are calculated and compared with the experimental data showing a very good performance. In this way the LPA stands as a very simple and reliable theoretical approximation to deal with inner-shell ionization of many-electron atoms by light ions, as far as total cross sections are concerned.

We also present here the results of employing the LPA in dealing with the dynamics of inelastic processes of dressed projectiles. Particularly we evaluate the simultaneous excitation of projectile and target electrons. The inelastic processes that take place in the target electrons represent the well-known antiscreening effect, usually referring to gases. Results show that projectile-electron-loss and excitation probabilities due to the collision with the ISE are comparable to those coming from the interaction with the FEG. In the case of electron loss of He^+ in Al, we obtain the equipartition of the FEG and ISE contributions at high velocities.

ACKNOWLEDGMENTS

We thank A. Arnau for useful discussions and comments on the subject. This work was partially supported by the Agencia Nacional de Investigación Científica y Tecnológica, Grant Nos. PICT 03-03579 and PICT99 03-06249, and by the Universidad de Buenos Aires, Grant No. UBACyT X044.

-
- [1] J. Lindhard, K. Dan. Vidensk. Selsk. Mat. Fys. Medd. **28**, 8 (1954).
 - [2] R.H. Ritchie, Phys. Rev. **114**, 644 (1959).
 - [3] J. Lindhard and A. Winther, K. Dan. Vidensk. Selsk. Mat. Fys. Medd. **34**, 4 (1964).
 - [4] D. Pines, *Elementary Excitations in Solids* (Benjamin, New York, 1964).
 - [5] A.L. Fetter and J.D. Walecka, *Quantum Theory of Many Particle Systems* (McGraw-Hill, New York, 1971).
 - [6] P.M. Echenique, F. Flores, and R.H. Ritchie, Solid State Phys. **43**, 229 (1990), and references within.
 - [7] L.C. Tribedi, V. Namal, M.B. Kurup, K.G. Prasad, and P.N. Tandon, Phys. Rev. A **51**, 1312 (1995).
 - [8] K. Sturm, E. Zaremba, and K. Nuroh, Phys. Rev. B **42**, 6973 (1990).
 - [9] I. Abril, R. Garcia-Molina, C.D. Denton, F.J. Perez-Perez, and N.R. Arista, Phys. Rev. A **58**, 357 (1998).
 - [10] D. Vernhet, J-P. Rozet, I. Bailly-Despiney, C. Stephan, A. Casimi, J-P. Grandin, and L.J. Dubé, J. Phys. B **31**, 117 (1998).
 - [11] J-P. Rozet, D. Vernhet, I. Bailly-Despiney, C. Fourment, and L.J. Dubé, J. Phys. B **32**, 4677 (1999).
 - [12] I. Gertner, M. Meron, and B. Rosner, Phys. Rev. A **18**, 2022 (1980).
 - [13] P. Sigmund, Phys. Rev. A **26**, 2497 (1982).
 - [14] Oddershede and J.R. Sabin, At. Data Nucl. Data Tables **31**, 275 (1984).
 - [15] P.M. Echenique, R.M. Nieminen, and R.H. Ritchie, Solid State Commun. **37**, 779 (1986).
 - [16] T. Kaneko, Phys. Rev. A **33**, 1602 (1986); **40**, 2188 (1989).
 - [17] J. Linhard and M. Scharff, K. Dan. Vidensk. Selsk. Mat. Fys. Medd. **27**, 15 (1953).
 - [18] J.D. Fuhr, V.H. Ponce, F.J. Garcia de Abajo, and P.M. Echenique, Phys. Rev. B **57**, 9329 (1998).
 - [19] A. Sarasola, J.D. Fuhr, V.H. Ponce, and A. Arnau, Nucl. Instrum. Methods Phys. Res. B **182**, 67 (2001).
 - [20] J. Calera-Rubio, A. Gras-Marti, and N.R. Arista, Nucl. Instrum. Methods Phys. Res. B **93**, 137 (1994).
 - [21] C.C. Montanari, M.S. Gravielle, V.D. Rodriguez, and J.E. Miraglia, Phys. Rev. A **61**, 022901 (2000).
 - [22] C.C. Montanari, J.E. Miraglia, and N.R. Arista, Phys. Rev. A **62**, 052902 (2000).
 - [23] M. Inokuti, J.L. Dehmer, T. Baer, and J.D. Hanson, Phys. Rev. A **23**, 95 (1981).
 - [24] E. Clementi and C. Roetti, At. Data Nucl. Data Tables **14**, 177 (1974).
 - [25] P.M. Echenique, R.H. Ritchie, and W. Brandt, Phys. Rev. B **20**, 2567 (1979).
 - [26] N.D. Mermin, Phys. Rev. B **1**, 2362 (1970).
 - [27] D. Isaacson, New York University Internal Report, 1975 (unpublished).
 - [28] N.R. Arista, Phys. Rev. A **49**, 1885 (1994).
 - [29] R.L. Wolke, W.N. Bishop, E. Eichler, N.R. Johnson, and G.D. O'Kelly, Phys. Rev. **129**, 2591 (1963).
 - [30] H.H. Andersen, J.F. Bak, H. Knudsen, and B.R. Nielsen, Phys. Rev. A **16**, 1929 (1977).
 - [31] D. Kahn, Phys. Rev. **90**, 503 (1953).

- [32] H. Sorensen and H.H. Andersen, Phys. Rev. B **8**, 1854 (1973).
- [33] P. Mertens, P. Bauer, and D. Semrad, Nucl. Instrum. Methods Phys. Res. B **15**, 91 (1986).
- [34] G. Martinez-Tamayo, J.C. Eckardt, G.H. Lantschner, and N.R. Arista, Phys. Rev. A **54**, 3131 (1996).
- [35] S.D. Santry and R.D. Werner, Nucl. Instrum. Methods Phys. Res. **188**, 211 (1981).
- [36] S.P. Moller, Nucl. Instrum. Methods Phys. Res. B **48**, 1 (1990).
- [37] D. Niemann, G. Konac, and S. Kalbitzer, Nucl. Instrum. Methods Phys. Res. B **118**, 11 (1996).
- [38] P. Mertens and P. Bauer, Nucl. Instrum. Methods Phys. Res. B **33**, 133 (1988).
- [39] E. Kührt, K. Lenkeit, and F. Täubner, Phys. Status Solidi B **66**, K131 (1981).
- [40] Sh.Z. Izmailov, E.I. Sirontinin, and A.F. Tulinov, Nucl. Instrum. Methods **168**, 81 (1980).
- [41] L.H. Andersen, P. Hvelplund, H. Knudsen, S.P. Moller, J.O.P. Pedersen, E. Uggerhoj, K. Elsener, and E. Morenzoni, Phys. Rev. Lett. **62**, 1731 (1989).
- [42] J.E. Valdes, J.C. Eckardt, G.H. Lantschner, and N.R. Arista, Phys. Rev. A **49**, 1083 (1994).
- [43] P. Mertens and Th. Krist, Nucl. Instrum. Methods Phys. Res. **194**, 57 (1982).
- [44] M. Luomajarvi, Radiat. Eff. **40**, 173 (1979).
- [45] Y. Kido and T. Koshikawa, Phys. Rev. A **44**, 1759 (1991).
- [46] K. Morita, H. Akimune, and T. Suita, J. Phys. Soc. Jpn. **25**, 1525 (1968).
- [47] A. Valenzuela, W. Meckbach, A.J. Keselman, and J.C. Eckardt, Phys. Rev. B **6**, 95 (1972).
- [48] H. Batzner, Ann. Phys. (Leipzig) **25**, 233 (1936).
- [49] V.A. Khodyrev, V.N. Mizgulin, E.I. Sirotinin, and A.F. Tulinov, Radiat. Eff. **83**, 21 (1984).
- [50] Y. Kido, Nucl. Instrum. Methods Phys. Res. B **24/25**, 347 (1987).
- [51] J.C. Eckardt and G. H Lantschner, Nucl. Instrum. Methods Phys. Res. B **93**, 175 (2001).
- [52] A. Ikeda, K. Sumimoto, T. Nishioka, and Y. Kido, Nucl. Instrum. Methods Phys. Res. B **115**, 34 (1996).
- [53] D.G. Arbo, M.S. Gravielle, J.E. Miraglia, J.C. Eckardt, G.H. Lantschner, M. Fama, and N.R. Arista, Phys. Rev. A **65**, 042901 (2002).
- [54] I. Orlic, C.H. Sow, and S.M. Tang, At. Data Nucl. Data Tables **56**, 159 (1994).
- [55] I. Orlic, Nucl. Instrum. Methods Phys. Res. B **87**, 285 (1994).
- [56] E. Braziewicz and J. Braziewicz, J. Phys. B **21**, 1537 (1988).
- [57] E. Braziewicz and J. Braziewicz, M. Pajek, T. Czyzewski, L. Glowacka, and W. Kretschmer, J. Phys. B **24**, 1669 (1991).
- [58] H. Paul, Nucl. Instrum. Methods Phys. Res. **192**, 11 (1982).
- [59] H. Paul and J. Muhr, Phys. Rep. **135**, 47 (1986).
- [60] G. Lapicki, J. Phys. Chem. Ref. Data **18**, 111 (1989).
- [61] H. Tawara, Y. Hachiya, K. Ishii, and S. Morita, Phys. Rev. A **13**, 572 (1976).
- [62] G. Basbas, W. Brandt, and R. Laubert, Phys. Rev. A **7**, 983 (1973).
- [63] G. Basbas, W. Brandt, and R. Laubert, Phys. Rev. A **17**, 1655 (1978).
- [64] K. Sera, K. Ishii, M. Kamiya, A. Kuwako, and S. Morita, Phys. Rev. A **21**, 1412 (1980).
- [65] W.M. Ariyasinghe, H.T. Awuku, and D. Powers, Phys. Rev. A **42**, 3819 (1990).
- [66] Y.P. Singh, D. Mitra, L. Tribedi, and P.N. Tandon, Phys. Rev. A **63**, 012713 (2000).
- [67] J.H. McGuire, N. Stolterfoht, and P.R. Simony, Phys. Rev. A **24**, 97 (1981).
- [68] R. Anholt, Phys. Lett. **114A**, 126 (1986).
- [69] E.C. Montenegro and W.E. Meyerhof, Phys. Rev. A **43**, 2289 (1991).
- [70] E.C. Montenegro and W.E. Meyerhof, Phys. Rev. A **46**, 5506 (1992).
- [71] E.C. Montenegro, W. S Melo, W.E. Meyerhof, and A.G. Pinho, Phys. Rev. Lett. **69**, 3033 (1992); Phys. Rev. A **48**, 4259 (1993).
- [72] E.C. Montenegro and T.J.M. Zouros, Phys. Rev. A **50**, 3186 (1994).
- [73] P.L. Grande, G. Schwiwietz, G.M. Sigaud, and E.C. Montenegro, Phys. Rev. A **54**, 2983 (1996).
- [74] G.M. Sigaud, F.S. Joras, A.C.F. Santos, E.C. Montenegro, M.M. Sant'Anna, and W.S. Melo, Nucl. Instrum. Methods Phys. Res. B **132**, 312 (1997).
- [75] A.B. Voitkiv, G.M. Sigaud, and E.C. Montenegro, Phys. Rev. A **59**, 2794 (1999).
- [76] C. J. Joachain, *Quantum Collision Theory* (North-Holland, Amsterdam, 1975), Vol. 1.
- [77] Mc Dowell and Colemann, *Introduction to the Theory of Ion-Atom Collisions* (North-Holland, Amsterdam, 1970).
- [78] S.T. Manson, Phys. Rev. A **5**, 668 (1972).
- [79] D.H. Madison, Phys. Rev. A **8**, 2449 (1973).
- [80] S.T. Manson, L.H. Toburen, D.H. Madison, and N. Stolterfoht, Phys. Rev. A **12**, 60 (1975).
- [81] A. Salin, J. Phys. B **22**, 3901 (1989).
- [82] J. Müller and J. Burgdörfer, Phys. Rev. A **43**, 6027 (1991).
- [83] M. Chevallier, A. Clouvas, N.V. de Castro Faria, B. Farizon Mazuy, M.J. Gaillard, J.C. Poizat, J. Remillieux, and J. Désesquelles, Phys. Rev. A **41**, 11 738 (1990).